

Wetenschappelijk ondersteuningsprogramma voor de normalisatie en technische regelgeving

**Reference materials for  
adequate porosity measurements**

**Eindverslag**

**N°NM/67/41  
NM/G2/42**

Federaal Wetenschapsbeleid

**Jan LUYTEN & Anita BUEKENHOUDT**

**Fabrice DE BARQUIN & Jean-François JOIRET**

VITO, MATERIALS TECHNOLOGY,  
Boeretang 200  
B-2400 MOL

WTCB-CSTC  
Avenue P.Holloffe 21  
B-1342 LIMELETTE

## **CONTENTS**

1	Introduction
2	Methology
2.1	Part 1
2.1.1	Synthesis of possible reference materials
2.1.2	Characterization of the candidate reference materials
2.1.3	Conclusions of part 1
2.2	Part 2
2.2.1	Selection of useful reference materials, analyzing methods and interpretation
2.2.1.1	The selection
2.2.1.2	Synthesis of the selected reference materials
2.2.1.3	Characterization of the selected reference materials
2.2.2	Application to practical problems.
2.2.3	Conclusions of part 2
3	Results of the project
4	Spreading and Valorization
5	Balance and Perspectives
6	Acknowledgement
7	References

## SUMMARY

Results of measurements of porosity, pore volume, pore size and pore size distribution, are always strongly dependent on the method and on the apparatus used to perform the measurements. Therefore, it is not only sensible to compare the measurements of different techniques on the same material, but to compare them also with measurements obtained on well-defined reference materials.

MIP (Mercury Intrusion Porometry) is a fast, cheap and reproducible method to study porous materials. Moreover, MIP measurements cover a large pore size range from 5 nm to 0.3 mm. Originally the objective of this Belgian Science Policy project was to develop MIP reference materials for this whole range of pore sizes. In view of the work already done by BAM, we have focused our efforts to pore sizes starting from 5  $\mu\text{m}$ .

The aim of the project was to develop:

- porous reference materials for MIP measurements
- a method to correct MIP measurements for their "bottle neck" behavior
- to applicate the method to practical problems

In the first year, porous materials were produced in a broad pore size range with different manufacturing techniques and analyzed with different techniques (MIP,  $\text{N}_2$ -adsorption/desorption, bubble point measurements, ...).

Sol gel techniques were used to produce flakes of pore sizes between 3 to 15 nm, a Reaction Bonded technique for pore sizes between 0.15 and 10  $\mu\text{m}$ , a powder agglomeration technique for pores till 100  $\mu\text{m}$  and for materials with still bigger pore sizes foam process techniques were used.

In the second year, the study was concentrated on materials with pore sizes between 5 and 100 $\mu\text{m}$ . These materials were extensively characterized with MIP and IA measurements.

Their reproducibility was demonstrated. A method was worked out to correct MIP measurements with a model based on image analysis of SEM pictures of the microstructure. The obtained techniques and their interpretation were demonstrated on materials with pore sizes between 5 and 100  $\mu\text{m}$  and on a few real brick materials with a well known pore structure.

There was an onset for the study of the watertransport behavior in brick materials and a start was made with the publication of the results.

Key words: Pore measurements, MIP, IA, reference materials

## Samenvatting

De resultaten van porositeitsmetingen, poriënvolume, poriëngrootte en poriëngrootte verdeling, zijn altijd sterk afhankelijk van de methode en van het apparaat waarmee de metingen worden uitgevoerd. Daarom, is het niet alleen zinvol om de metingen te vergelijken met verschillende technieken op éénzelfde monster, maar ook om ze te vergelijken met metingen uitgevoerd op wel gedefinieerde referentie materialen.

MIP (Mercury Intrusion Porometry) is een snelle, goedkope en reproduceerbare methode om poreuze materialen te bestuderen. Daarbij, bestrijken MIP metingen een breed poriëngrootte gebied nl van 5 nm tot 0.3 mm. Origineel was het objectief van dit Federaal Wetenschapsbeleid project om MIP referentie materialen te maken voor het ganse poriëngrootte gebied. In het licht van het werk wat al gedaan werd op BAM, werden de inspanningen uiteindelijk gefocust op poriëngrootte beginnend van 5  $\mu\text{m}$ .

De doelstellingen van dit normalisatie project kunnen als volgt worden samengevat:

- 1. aanmaken van poreuze referentiematerialen voor Hg-porositeitsmetingen (MIP).
- 2. Het ontwikkelen van een methode om deze MIP-metingen te corrigeren voor hun "bottle neck"-gedrag.
- 3. Deze methode te demonstreren voor enkele praktische problemen.

In het eerste jaar werden poreuze materialen geproduceerd in een breed poriëngrootte gebied met verschillende aanmaaktechnieken en geanalyseerd met een waaier van technieken (MIP, N<sub>2</sub>-adsorptie/desorptie, Bubble point metingen....

Sol gel technieken werden gebruikt voor het bekomen van flakes met poriën tussen 3 en 15 nm, een Reaction Bonded techniek voor poriën tussen 0.15 en 10  $\mu\text{m}$ , een poeder agglomeratie techniek voor poriën tot 100  $\mu\text{m}$  en voor de materialen met nog grotere poriën werden schuim aanmaaktechnieken ingeschakeld.

In het tweede jaar was de studie geconcentreerd op materialen met poriëngrootte tussen 5 en 100  $\mu\text{m}$ . Deze materialen werden uitvoerig gekarakteriseerd met MIP- en beeldanalyse (IA) metingen. Hun reproduceerbaarheid werd aangetoond. Een methode werd uitgewerkt waarbij de MIP-metingen werden gecorrigeerd met een model gebaseerd op beeldanalyses van SEM beelden van de microstructuur. De bekomen technieken en hun interpretatie werden gedemonstreerd op materialen met poriëngrootte tussen 5 en 100  $\mu\text{m}$  en op een paar echte bouwmaterialen met een wel bekende poriën structuur.

Er was tevens een aanzet voor de studie van het watertransport gedrag in bouwmaterialen en een start werd gemaakt met het publiceren van de resultaten.

Key words: Pore measurements, MIP, IA, reference materials

## RESUME

Les résultats de mesures de porosité, de volume des pores, de dimension de pores et de distribution des dimensions des pores sont toujours fortement dépendants de la méthode et de l'appareillage utilisés pour la réalisation des mesures. Par conséquent, il n'est pas seulement sensé de comparer les mesures selon différentes techniques sur le même matériau mais également de les comparer avec des mesures obtenues sur des matériaux de référence bien définis.

La MIP (Mercury Intrusion Porometry) est une méthode rapide, peu coûteuse et reproductible pour étudier les matériaux poreux. De plus, les mesures MIP couvrent une large gamme de dimensions de pores (de 5 nm à 0.3 mm). Initialement, l'objectif de ce projet de la Politique scientifique fédérale était de développer des matériaux de référence MIP pour cette entière gamme de dimensions de pores. Etant donné le travail déjà accompli au BAM, nous avons concentré nos efforts aux dimensions de pores à partir de 5  $\mu\text{m}$ .

L'objectif du projet était de développer:

- des matériaux poreux de référence pour des mesures MIP
- une méthode de correction des mesures MIP pour leur comportement "bouteille d'encre"
- d'appliquer la méthode à des problèmes pratiques.

Durant la première année, les matériaux poreux furent produits dans une large gamme de dimension de pores avec différentes techniques de fabrication et analysés au moyen de différentes techniques (MIP,  $\text{N}_2$ -adsorption/désorption, mesures bubble point, ...).

Furent utilisées les techniques *Sol gel* pour produire des éprouvettes aux dimensions de pores entre 3 et 15 nm, une technique *Reaction Bonded* pour les dimensions de pores entre 0.15 et 10  $\mu\text{m}$ , une technique *d'agglomération de poudre* pour les pores jusqu'à 100  $\mu\text{m}$  et les techniques *foam process* pour les matériaux avec des dimensions de pores encore plus grandes.

Durant la seconde année, l'étude était concentrée sur des matériaux avec des dimensions de pores comprises entre 5 et 100  $\mu\text{m}$ . Ces matériaux furent largement caractérisés par des mesures MIP et par analyse d'images.

Leur reproductibilité a été démontrée. Une méthode a été établie afin de corriger les mesures par MIP avec un modèle basé sur l'analyse d'images de la microstructure obtenue au SEM. Les techniques obtenues et leur interprétation furent démontrées sur des matériaux avec des pores de dimensions comprises entre 5 et 100  $\mu\text{m}$  et sur plusieurs types de briques de terre cuite dont la structure poreuse est bien connue.

Des applications pratiques furent réalisées sur le comportement des briques de terre cuite vis-à-vis du transfert de l'eau et les premiers résultats furent publiés.

.

Mots clé: mesures de pores, MIP, IA, matériaux de référence

## **1 INTRODUCTION**

Results of measurements of porosity, pore volume, pore size and pore size distribution, are always strongly dependent on the method and on the apparatus used to perform the measurements. Therefore, it is not only sensible to compare the measurements of different techniques on the same material, but to compare them also with measurements obtained on well-defined reference materials.

MIP (Mercury Intrusion Porometry) is a fast, cheap and reproducible method to study porous materials. Moreover, MIP measurements cover a large pore size range from 5 nm to 0.3 mm. Originally the objective of this Belgian Science Policy project was to develop MIP reference materials for this whole range of pore sizes. In view of the work already done by BAM, we have focused our efforts to pore sizes starting from 5  $\mu\text{m}$ .

In a first part of the project the MIP results on the obtained reference materials are compared with other pore size analyzing techniques, and especially IA (Image analyze). Indeed, with the arrival of strong hardware and computer processing of images, IA becomes an important additional tool for the study of pores. It gives especially the possibility to quantify the morphological aspects of the pores. MIP does not consider these morphological aspects in a pore size measurement, because all the data are interpreted by a model based on cylindrical pores.

Therefore, it is the main objective of this project to be able to correct the pore size distribution obtained by MIP measurements for their known "bottle neck" behavior, by IA. In this way, better exploitable measurement data by MIP can be obtained.

This objective was extensively worked out in part two, especially for materials with maximum pore size of 5  $\mu\text{m}$  and 50  $\mu\text{m}$ , in view of the considerations of the steering committee.

## **2 METHODOLOGY**

### **2.1 Part 1**

#### **2.1.1 Synthesis of possible porous reference materials**

We concentrated our work on porous ceramic materials because these materials have a high E-modulus and are therefore very useful as reference materials. Originally it was the aim to develop porous reference materials for the whole range of pore size covered by MIP, meaning from 5 nm to 0.3 mm. It is clear that such large spectrum of pore sizes can not be realized by only one synthesis route.

Therefore we have chosen the following manufacturing routes for the different pore size ranges:

1.  $\gamma$ - $\text{Al}_2\text{O}_3$  flakes produced by the sol-gel method [1,2]. The flow chart of this procedure can be found in figure 1. Depending on the calcination temperature, we can produce materials with a sharp pore size maximum between 5 and 10 nm. By doping with large atoms as La, the pore-size range can be increased to about 15 nm. In the project, the calcination step was chosen so that materials with a maximum pore size of respectively 5 and 10 nm were obtained (RM 1 and RM 2).  
Due to the sol-gel approach, these materials can only be produce as flakes.

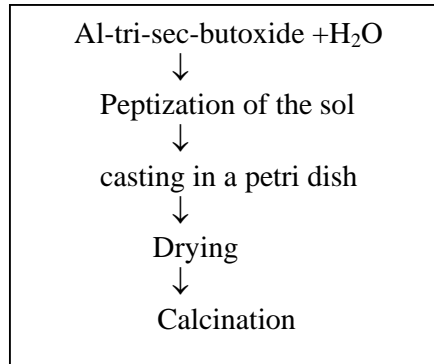


Figure 1: Flow chart of the synthesis of  $\gamma$ - $\text{Al}_2\text{O}_3$  flakes.

2.  $\alpha$ - $\text{Al}_2\text{O}_3$  manufactured by a porous Reaction Bonded Alumina (RBAO) technology, developed at Vito [3,4]. The flow chart of this processing route is described in figure 2. Depending of the milling time of the starting mixture Al/ $\text{Al}_2\text{O}_3$ , this technology can supply materials with sharp pore size maxima between 0.15 and 10  $\mu\text{m}$ . We decided to produce materials with pore sizes of 0.2, 2 and 5  $\mu\text{m}$  (RM 3, 4 and 5). The specimens can be shaped in pellets, discs and tubes, for characterization at Vito, or in cylinders with well determined dimensions, for characterization at WTCB/CSTC

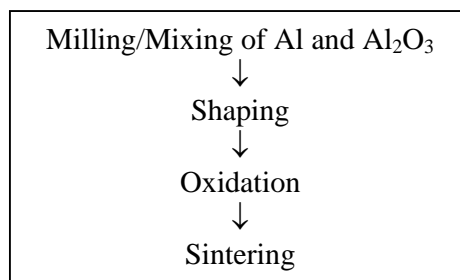


Figure 2: Flow Chart of the synthesis of Reaction Bonded Alumina.



3. Highly porous  $\alpha$ -Al<sub>2</sub>O<sub>3</sub> produced by the normal powder technology, but starting from a mixture of 2 powders with different particle size. The flow chart of this synthesis is shown in figure 3. One of the powders of the mixture is a spray dried powder, from which we used only the fraction between 180 and 250  $\mu$ m, obtained by sieving, after sintering. The second powder is a fine, high sinter active powder, which was added in proportions of 5 to 10 wt%. With this method, materials with a maximum pore size of 50  $\mu$ m (RM 6) were obtained.

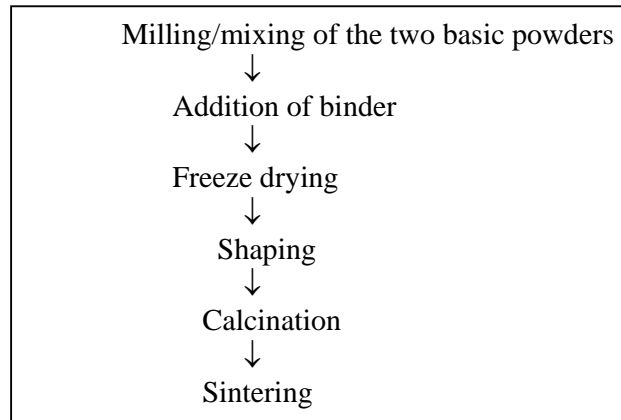


Figure 3: Flow chart of the synthesis of strong porous  $\alpha$ -alumina.

4.  $\alpha$ -Alumina ceramic foams produced by gel casting [5,6]. The flow chart of this synthesis route is given in figure 4. This manufacturing route produced materials with pores in the mm range. The calcination and sintering step are chosen in that way that we get pores in the range of 0.3 mm (RM 7). With this manufacturing route, though, we have difficulties to produce a material with a narrow pore size distribution. A fraction of the pore size distribution is even above 300  $\mu$ m and thus not measurable with MIP. Therefore, we have stopped the synthesis of these materials for this project.

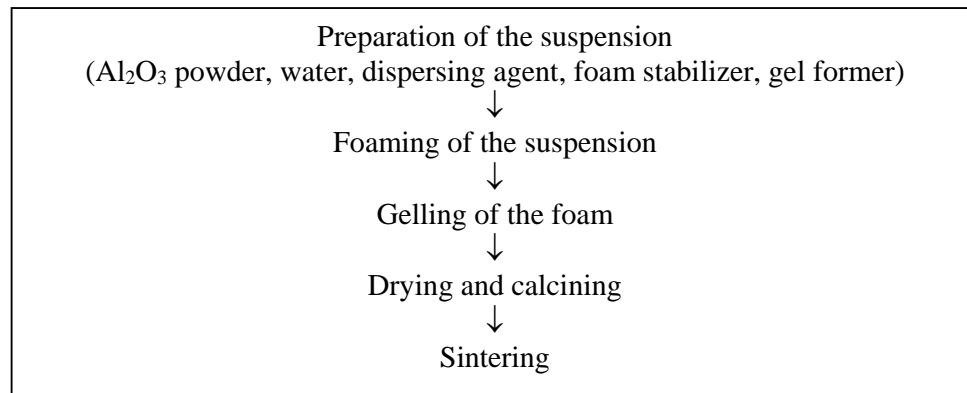


Figure 4: Flow chart of the synthesis of Alumina foam structures.

## 2.1.2 Characterization of the candidate reference materials [7-11]

### Characterization at Vito

At Vito the pore structure of the candidate reference materials were characterized with the following techniques.

MIP (Quantachrome)

Bubble point measurements

Tortuosity measurements (home-made apparatus)

N<sub>2</sub>-Adsorption/desorption measurements (Quantachrome)

Surface roughness measurements with a laserprofilometer.

FESEM (Jeol)

#### MIP results

MIP measures the open pores of the porous material. The measurements are performed on flakes of RM 1 and RM 2, and on cylinders of RM 3, 4, 5, 6 and 7.

The dimensions of the cylinders are: height = 5 mm, diameter = 20 mm. The following table 1 summarizes the results of measurements done on half of such a cylinder of each candidate reference material.

The pores of RM 1 were a little too small to allow measurements with MIP: no mercury intrusion could be found. The MIP apparatus of Vito can only be used starting from pore sizes of 6 to 7 nm.

Table 1 : MIP measurements on candidate reference materials.

Reference materials	Max-pore size (µm)	Porosity (vol%)
RM 1	No intrusion	No intrusion
RM 2	0.01	53
RM 3	0.2	29
RM 4	2	30
RM 5	5	34
RM 6	50	36
RM 7	>300	>?

The MIP intrusion curves and the pore size distributions can be found in appendix 1.

As already mentioned, RM 6 and RM 7 have very large pore size distributions.

#### Bubble point measurements

Bubble point measurements, frequently used for membranes, are based on the permeation of a gas through a porous specimen which is filled with a liquid. The measurement of the pressure at which a first gas bubble passes through the specimen, is a measure of the biggest pore of the material.

The measurements were performed on tubes, filled with a liquid with a strong wetting behavior, Porofil. The pore-size range measured in this way ranges from 0.06 to 65 µm.

For this project bubble point measurements were performed on tubes from RM 3, 4 and 5. The other candidate reference materials have pore sizes outside this range and could therefore not be tested by this method.

The results are shown in table 2. It is clear from this table that there is no correlation with the MIP measurements of table 1 : the bubble point measurements give too low values.

Table 2: Bubble point measurements on candidate references materials.

Reference material	Bubble point pressure (bar)	Biggest pore ( $\mu\text{m}$ )	remarks
RM 3	>10	<0.07	No permeation
RM 4	1.02	0.63	
RM 5	0.25	2.61	

### Tortuosity measurements

The tortuosity  $\tau$  is a measure of the non-cylindrical, winding behavior of the pores. For a perfect cylindrical pore  $\tau = 1$ . In real porous materials  $\tau > 1$ . The tortuosity can be calculated from the resistance of an electrolyte through a disc shaped specimen:

$\tau = (\varepsilon \times \rho) / \rho_0 \times 100$  . Hereby  $\varepsilon$  is the porosity of the disc,  $\rho$  the specific resistance of the disc in the electrolyte ( $\Omega\text{cm}$ ) and  $\rho_0$  the specific resistance of the electrolyte ( $\Omega\text{cm}$ ). As electrolyte we use here an aqueous solution of KOH 31 wt % at 30°C.

The specific resistance is in that case 1.59  $\Omega\text{cm}$ . Table 3 gives the measurements for discs with a diameter of 5.5 cm and produced with RM 3, 4, 5.

Table 3 : Tortuosity measurements on candidate reference materials.

Reference material	Porosity (vol%)	$\rho$	$\tau$
RM 3	46	6.02	1.79
RM 4	30	9.13	1.81
RM 5	35	6.24	1.42

For RM 4 and RM 5 there is a good correlation between the porosity measured by this method and MIP. This is not the case for RM 3. Probably this is caused by the different dimensions and shapes of the samples. This was confirmed by further MIP measurements, see table 5.

### N<sub>2</sub>-adsorption/desorption measurements

This method screens open pores from 0.5 to 50 nm. Therefore, this measurement has only sense for the two first candidate reference materials. They were performed on flakes of RM 1 and RM 2. The results are shown in table 4. The result of RM 2 was comparable with the result obtained with MIP.

Table 4: N<sub>2</sub>-adsorption/desorption measurements on candidate reference materials.

Reference materials	Max.pore size (nm)	Porosity (vol %)
RM 1	5	55
RM 2	10	53

#### Dependence of MIP results on the sample size

As already mentioned, it was suspected that the MIP measurements are influenced by the sample dimensions and the sample shape. Therefore, MIP measurements were performed on the same reference materials, but shaped differently. Table 5 shows the results of this study. To compare, MIP results of WTCB/CSTC were added in the table.

Table 5: MIP measurements on samples with different shape and volume.

Reference material	Shape and dimensions of the sample	Volume MIP sample (cc)	Porosity (vol. %)
RM3			
Sample 1	Pellet (diameter= 2 cm, height= 0.5 cm)	0.67	29
Sample 2	Cylinder(diameter= 1 cm, height= 2 cm)	0.76	34
Sample 3	Disc (d=5.5cm, thickness=0.4 cm)	0.49	41
WTCB	Cylinder (diameter= 1 cm, height=2 cm)	1.48	41
RM5			
Sample 1	Pellet (diameter= 2 cm, height= 0.5 cm)	0.64	34
Sample 2	Cylinder(diameter= 1 cm, height= 2 cm)	0.64	38
Sample 3	Disc (d=5.5cm, thickness=0.4 cm)	0.52	35
WTCB	Cylinder (diameter= 1 cm, height=2 cm)	1.48	35

These results demonstrate the importance of using standard specimens for MIP measurements.

#### **Characterization of the candidate reference materials at WTCB**

The different alumina samples produced by Vito for characterization at WTCB, are cylinders with a diameter of 9.7 mm and with a height of 20mm. It concerns RM 3, 4, 5, and 6. They were analyzed with MIP and SEM.

#### MIP results

The MIP measurements are performed here with a Micromeritics apparatus type Autopore II. The maximum pressure obtained with this apparatus, is 4000 bar. As a consequence, pores with diameters from 350 to 0.0035 $\mu$ m can be measured.

For interpretation of the results the standard properties of mercury, as given by the producer, were used (idem for Vito):

Contact angle Hg: 142°

Surface stress Hg: 485 dynes/cm<sup>2</sup>

Density Hg: 13.5335 g/ml

The first results are summarized in Table 6. It shows the results of different cylindrical samples of the same dimensions of each candidate of the reference material. The samples were used as a whole. Figures of the measurements are added in appendix 2.

Table 6: MIP measurements at WTCB.

Reference material	Porosity (Vol%)	Mean pore size diameter (µm)	Matrix density (g/ml)
type RM3			
000-336	40.70	0.15	3.80
average	40.70	0.15	3.80
type RM4			
000-327	30.98	1.67	3.96
000-334	30.90	1.7	3.95
average	30.94	1.69	3.96
type RM5			
000-331	35.62	4.13	4.06
000-332	36.02	4.31	4.08
000-378	32.99	4.19	3.93
average	34.88	4.21	4.02
type RM6			
000-328	29.84	23.10	3.77
000-333	26.61	20.29	3.67
000-367	30.90	22.51	3.84
000-369	29.09	23.67	3.74
000-370	28.99	24.10	3.74
average	29.08	22.73	3.75

The table shows the distribution of the porosity of samples of the same shape and dimensions. Deviations of 5 to 10 % are possible. On the contrary, nearly no differences are seen for the pore size distribution of similar samples.

#### Results of SEM analyses

The analyses with the scanning electron microscope are performed on samples polished after vacuum impregnation with an epoxy resin. Sections are made perpendicular on the cylinder axis, if not mentioned otherwise.

The images are obtained with a detector for back-scattered electrons. The images are formed with 256 grey levels (the grey levels are dependent of the mean atomic weight  $Z$  of the element). The resolution in the grey-levels is about  $\pm 0.1 Z$ .

Due the light atomic weight of the resin (composed of C and O-atoms), the pores are always dark, and therefore well distinguished from the matrix material, which is middle grey. You can find an example of such micrograph in figure 5.

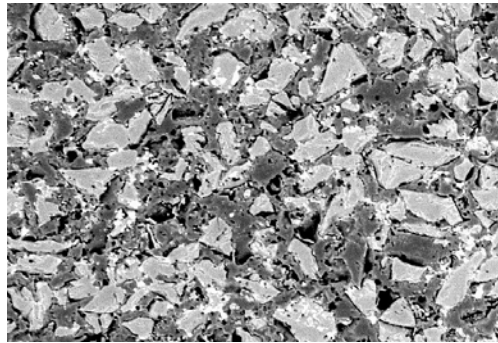


Figure 5: Example of a SEM-image of RM5. The pores are dark grey.

An image analysis system is connected with the SEM and allows a quantitative interpretation of the measurements. The system used is of the type Kontron KS400.

The measurements of the total porosity by image analysis (IA) are performed by counting the pixels occurring in the phase to be measured, here, the dark regions filled by resin. The selection of the desired phase is performed by a *thresholding* operation [12]. This aims at identifying that part of the grey-level histogram of a total image, corresponding to the phase to be measured. Figure 6 shows an example of such a grey-level histogram for a RM5 sample. On the x-axis are indicated the 256 grey levels are indicated (from 0 for black, to 255 for white) and the y-axis shows the percentage of pixels of the corresponding grey level.

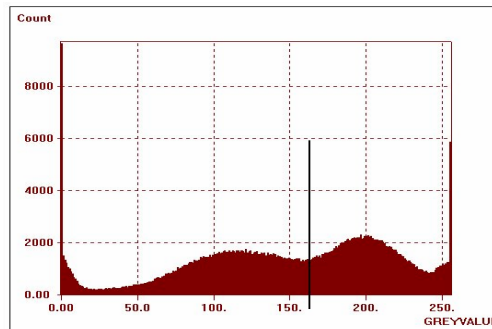


Figure 6: Example of a histogram with grey levels of a SEM image.

The distribution is typically bimodal: a peak for the pore-phase, and one for the material-phase. The thresholding operation identifies the grey levels corresponding with the pore phase, starting from 0 to about 140 (the separation of both distributions). All the pixels corresponding to this category are then colored white, and the remaining part is turned to black.

In this way, we obtain a binary image which can be easily measured by the image analysis system. Figure 8 shows the result for this operation starting from the micrograph of figure 7.

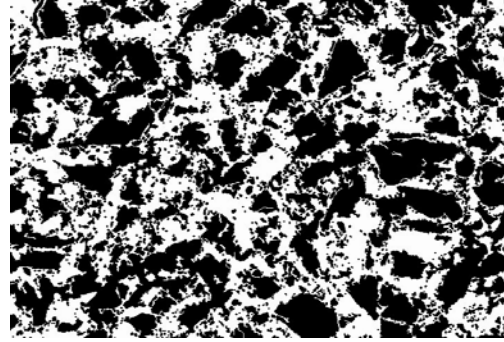
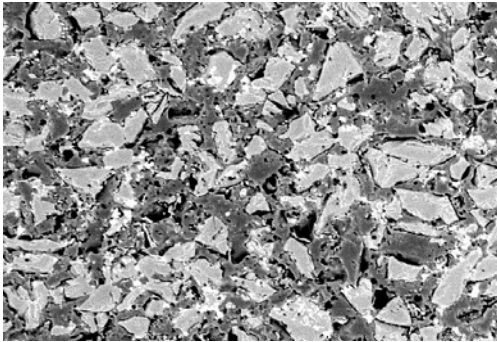


Figure 7: Original SEM image.

Figure 8: Binary image of figure 7.

By dividing the area of the phase selected to the total area of the image, we can consequently determine the content of pores corresponding to the field of observation.

In order to obtain a measure of porosity for the whole sample, it is necessary to take measurements of porosity on several fields of observation.

The optimal number of measured fields in order to know the porosity of the sample, with an error and an uncertainty fixed, can be given using statistical methods.

The objective is to find a confidence interval for  $\mu$  (median porosity of the whole sample) with specified confidence coefficient  $1-\alpha$  ( $0 < \alpha < 1$ ) and span  $2\varepsilon$  ( $0 < \varepsilon < \alpha$ ) :

$$P[\bar{x} - \varepsilon \leq \mu \leq \bar{x} + \varepsilon] \geq 1 - \alpha$$

with  $\mu$  : real median porosity of the sample.

$\bar{x}$  : median porosity measured.

$\varepsilon$  : error on the measurement.

$\alpha$  : degree of uncertainty [0;1].

The statistical method of Stein [13,14] allows, using information provided by a first pilot sample of measurements, to determine the additional number of measurements required to obtain the above-mentioned confidence interval.

The method is divided in two phases :

1. Start with a pilot sample size, let:

-  $n_0$  the number of fields measured,

-  $x_1, \dots, x_{n_0}$  the measures of porosity of these fields,

-  $\bar{x}_0 = \sum_{i=1}^{n_0} \frac{x_i}{n_0}$  the mean,

-  $s_0^2 = \frac{\sum_{i=1}^{n_0} (x_i - \bar{x}_0)^2}{n_0 - 1}$  the unbiased standard deviation.

2. Compute the required number of measures :

$$n = \max \left( n_0, \frac{t_{(n_0-1, 1-\alpha/2)}^2 s_0^2}{\varepsilon_r^2 \bar{x}_0^2} \right)$$

with  $t_{(v, p)}$  = quantile of probability  $p$  of the student's distribution with  $v$  degrees

of freedom.

$\varepsilon_r$  = relative error.

Thus, at the end of the  $n_0$  (30 for example) measured fields of observation,

If  $n \leq n_0$ , the  $n_0$  first measurements are sufficient;

If  $n > n_0$ ,  $(n-n_0)$  supplementary measures should be taken.

Then, at the end of these  $n$  measurements, the average of those provides the total porosity of the sample with a limited relative error  $(\varepsilon_r * 100)\%$  in  $((1-\alpha) * 100)\%$  of the cases.

Also let us specify that the method of Stein presented above is valid only if the following assumptions are satisfied:

- Independence of observations/measures carried out.

- Observations/measures distributed according to a Normal law.

For sufficiently homogeneous samples (as it is the case in fact), these assumptions are checked in practice.

In addition, to minimize the effect of possible local variations of porosity, the fields of observation are selected randomly on the whole surface of the sample.

Moreover, measurements taken in great number on some samples revealed that the distribution of measurements followed indeed a Normal law.



Table 7: Porosity measurements on candidate reference materials by IA.

Reference material	Number of image measured	Mean porosity (vol%)	Standard deviation (vol%)
RM3			
RM4	100	43.73	2.61
RM5	400	44.65	1.76
RM6 (⊥ cylinder axis)	35	50.85	5.51
RM6 (   cylinder axis)	100	43.01	3.58

From this table, it is clear that the porosities, measured with IA, are much larger than those measured by MIP. The deviations are as big as 10%. It is expected that the pore size of the MIP measurements and the IA measurements is different, due to the bottle neck effect. But a difference in porosity is not expected. The reasons for this have been studied further in Part 2.

#### Measurements of the surface roughness by optical interference microscopy

The apparatus used is of the type "WYCO surface profiler" and is based on reference techniques. The apparatus allows to determine the standard roughness parameters as Ra (mean roughness) and Rq (root mean square roughness) [15] with a vertical resolution of 3 nm.

Measurements were done on RM3 (see appendix 2) and give as results Ra = 2.89µm and Rq = 3.66.

### **2.1.3 Conclusions**

- MIP measurements of Vito and WTCB are comparable, but the porosities of the same reference materials show clear differences, especially when they were shaped differently. Because it is necessary to produce other shapes for the other analyzing techniques (bubble point, tortuosity,...), it is difficult to correlate their results with the results obtained by MIP. The pore-size distribution on the other hand is well reproducible.
- IA measurements indicate a substantial higher porosity than MIP.

## **2.2 Part 2**

### **2.2.1 Selection of useful reference materials, analyzing methods and interpretation**

#### **2.2.1.1 The selection**

Prof. K. Meyer (BAM) has advised us to concentrate on reference materials with rather large pore sizes (conclusion of the November meeting).

In view of the research done at BAM on reference materials (concentrated on pores  $\leq 5 \mu\text{m}$ ), we limited our work to materials with a maximum pore size of  $5 \mu\text{m}$  and  $50 \mu\text{m}$ . The pore size of  $5 \mu\text{m}$  was chosen, to be able to compare with the BAM  $5 \mu\text{m}$  candidate reference material (work not fully completed).

#### **2.2.1.2 Synthesis of the selected reference materials**

The  $5 \mu\text{m}$  reference material was made using the method described in Part 1, 2.1.1. From the characterizations done in part 1 we know that this reference material can be synthesized in a reproducible way. The material with a maximum pore size of  $50 \mu\text{m}$  on the other hand, had to be further optimized. We give here the finally obtained manufacturing flow sheet (figure 9). Later on we used the same procedure also for the processing of other porous materials with a pore size of about  $100 \mu\text{m}$  for further evaluation of the obtained MIP-IA interpretation procedure.

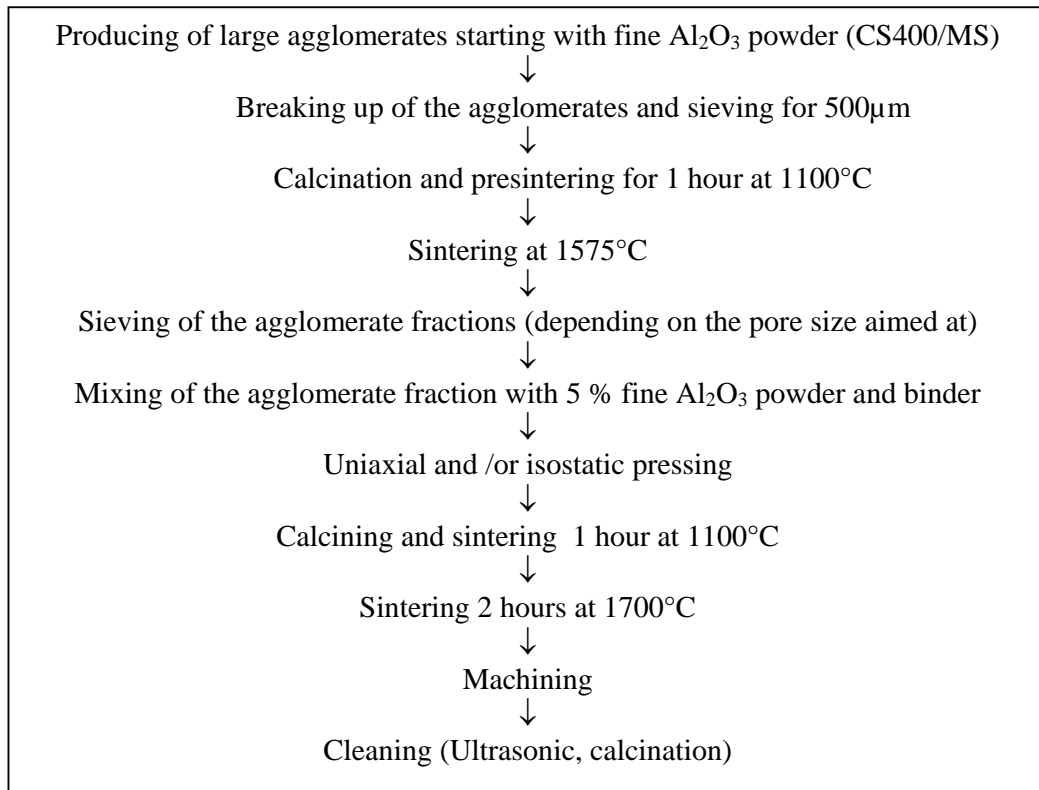


Figure 9: The processing route for materials with pore sizes larger the  $10\ \mu\text{m}$ .

### 2.2.1.3 Characterization of the selected reference materials

#### Reference material with pore size of $5\ \mu\text{m}$

##### Comparison BAM-VITO $5\ \mu\text{m}$

Figure 10 shows a comparison of the MIP results on the Vito and the BAM  $5\ \mu\text{m}$  candidate reference material. The figure shows a difference in pore volume, but the maximum pore size and the pore size distribution are nearly the same.

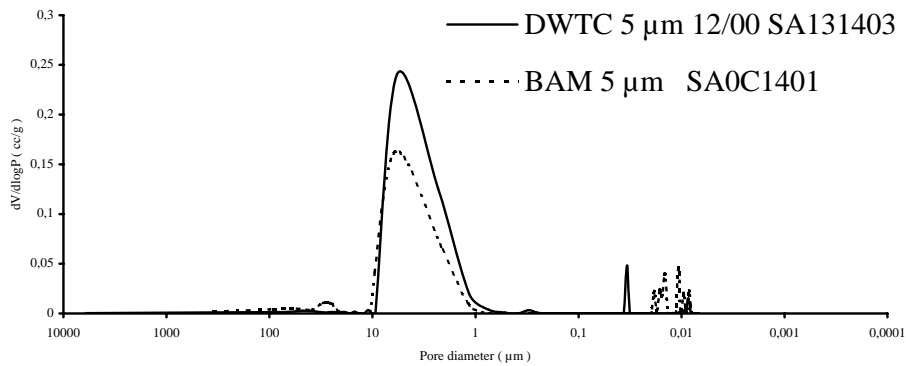
Pore distribution BAM - VITO 5  $\mu\text{m}$ 

Figure 10: Comparison pore distribution of BAM and Vito 5  $\mu\text{m}$  reference material.

MIP-measurements Vito/WTCB for 5  $\mu\text{m}$

In Part 1, differences were measured between MIP porosities measured at WTCB and at Vito. Therefore, the differences of both MIP apparatus and the way of measuring were studied. Measurements on materials of the same batch, shaped in the same way, and done on a same material volume (Stem), show a nearly constant difference of only 1 % (Table 8). This remaining small difference can be explained by a lower maximum pressure of the Quanta Chrome apparatus (Vito), compared to the Micromeritics one (WTCB). We want to mention also that SEM pictures of the powder agglomerates used to synthesize the 5  $\mu\text{m}$  materials, show that these materials are homogeneous and without holes.

Table 8: MIP measurements on the same material volume.

WTCB	Vito
39.5	38.7
39.4	38.4
39.3	38.3
40.3	38.7
39.0	37.6
39.2	38.6
39.0	
Mean $39.4 \pm 0.5$	Mean $38.4 \pm 0.5$

The differences between pore volumes of MIP and IA.

As explained also in Part 1, it is expected that the pore size of the MIP measurements and the IA measurements is different, due to the bottle neck effect. Therefore we expected a difference in pore size, but not in pore volume. Nevertheless we have still an unexplainable difference of 5% in pore volume between MIP and IA.

### Roughness measurements

Roughness measurements were done on the 5  $\mu\text{m}$  reference materials of Vito and BAM. The mean roughness parameter  $R_a$  is about 4.5  $\mu\text{m}$  for the BAM material, and about 5.2  $\mu\text{m}$  for the Vito material. Both figures are found, as well for surface measurements (1mmx1mm), as for line measurements in different directions. Surface irregularities of 40 to 50  $\mu\text{m}$  can be found on both surfaces. The mean roughness parameter clearly correlates with the maximum pore diameter of the samples. A similar correlation was already seen on the preliminary roughness measurements mentioned in part I.

### Coupling of MIP and IA for correcting the pore size distribution of MIP

The images furnished by SEM can be treated by IA to determine the pore size distribution and correct the bottle neck effect of MIP.

A first possible application of the IA could consist on extracting, from the porous mass, the porous objects according to some criteria of form and/or surface and to characterize them by using a representative diameter.

The separation between main pores and their channels is based on a general shape manipulation leading to classify the porosity in 2 categories : “rounded pores” and “pore channels” – see figure 11 below.

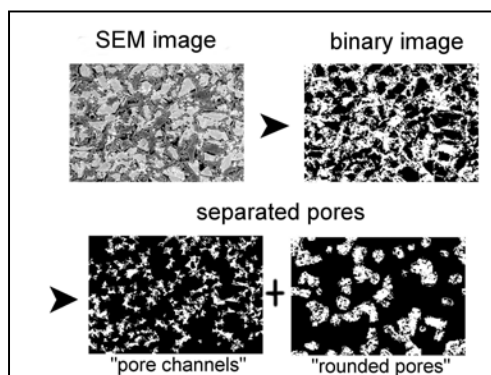


Figure 11: Classification in “rounded pores” and “pore channels”

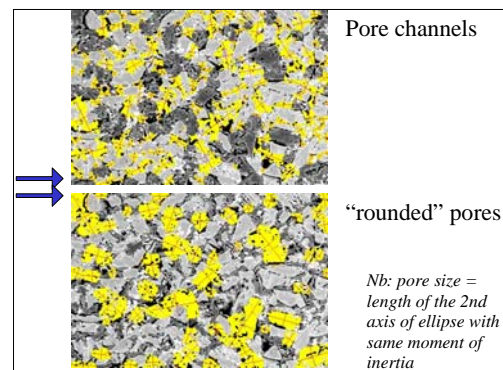


Figure 12: IA further technique.

Once this separation carried out, it is possible to characterize the objects extracted from this "porous mass" by using an equivalent diameter [16]. Because an ellipse is likely to modelise the porous channels satisfactorily as well as the rounded pores by degeneration in a circular form, the choice of the characteristic diameter for a porous "object" was made over the length of the second axis (smallest) of the ellipse having the same moment of inertia as the object (Figure 12).

This technique (called “IA” further) uses specific image analysis functions in order to achieve this separation. It’s highly dependent on the parameters chosen and, consequently, highly subjective [17].

Another technique, much more objective than the former, to eliminate this bottle neck effect consists in simulating the intrusion of mercury on the images furnished by SEM, while preserving an identical criterion with regard to the assignment of a pore volume to a class of particular diameter.

This approach makes it possible on the one hand to simulate the invasion of the mercury introduced under various pressures by the edges of the sample and thus to reproduce the distribution curve of the pore diameters provided by MIP (see "MIP Simulation" : figure 13).

In addition, it also makes it possible to provide the true distribution curve of the pore diameters by introducing into each porous volume the spheres with maximum diameter (see "MIP Correction" : figure 14).

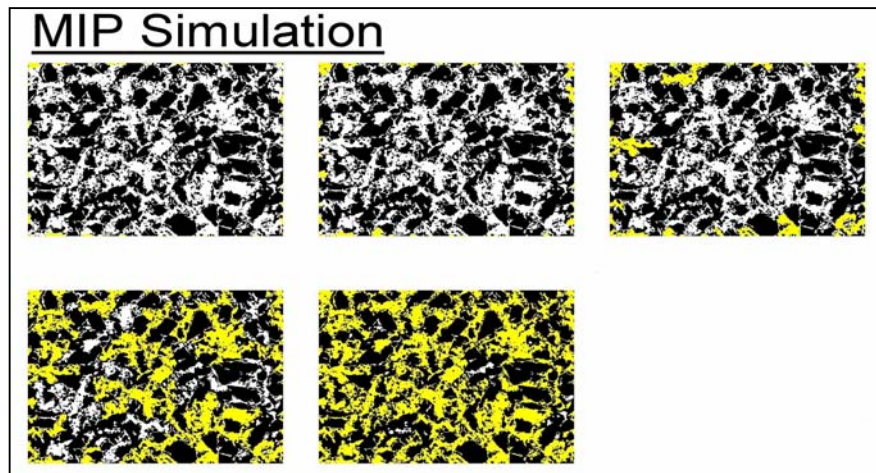


Figure 13: MIP simulation

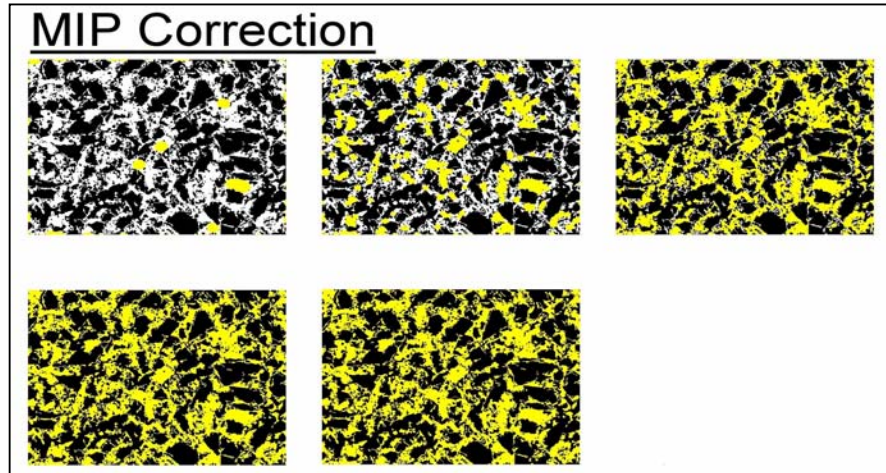


Figure 14: MIP Correction

The comparison of pore size distribution, for the Vito 5  $\mu\text{m}$  porous reference material, between MIP and IA is given in figure 15 below. Excellent correlation is found between the mean pore diameter measured by MIP and the one given by IA for the “channel” pores. This confirms the fact that the intrusion curve of MIP gives the distribution of the pore accesses (channels) and not of the whole porosity [18].

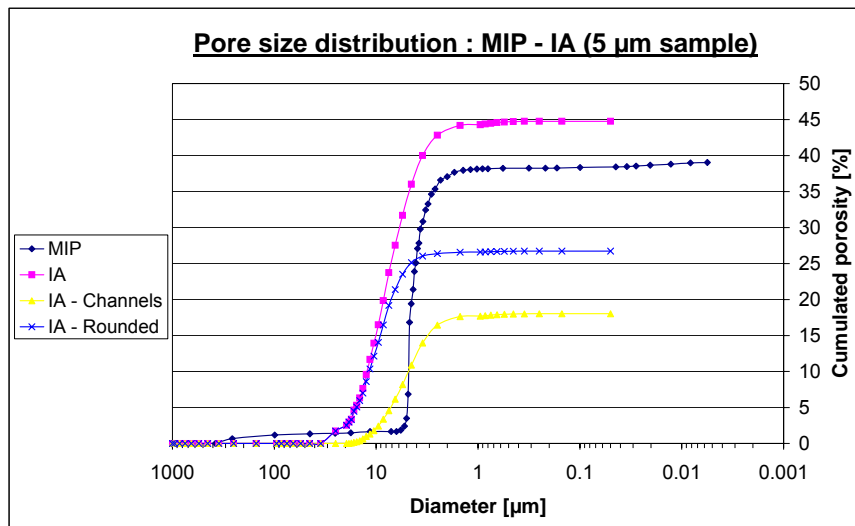


Figure 15: The comparison of the pore size distribution between MIP, IA, IA-channels and IA-rounded for a 5  $\mu\text{m}$  sample.

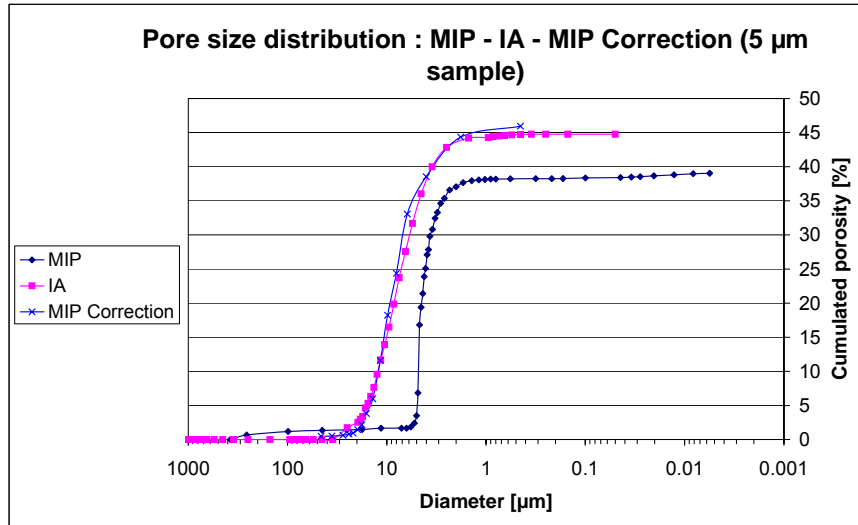


Figure 16: The comparison of pore size distribution between MIP, IA and MIP correction for a 5 µm sample.

The comparison of pore size distribution, for the Vito 5 µm porous reference material, between MIP, IA and MIP Correction (released at magnitude 200x) is given in figure 16 above. A good correlation is found between IA and MIP Correction (based on SEM Images).

### Conclusions

- The material with pores of 5 µm produced at Vito is very comparable with the 5 µm porous reference material which is under development at BAM.
- The difference in pore volume between the MIP measurements of Vito and WTCB is measured to be constant, and about 1 %. It can be explained by differences in apparatus.
- An IA method was developed to correct the pore size measured by MIP for the bottleneck effect. The efficiency of this method was checked with the 5 µm material of Vito.

### Reference materials with pore sizes of 50µm (and larger then 5 µm)

The materials produced as indicated in figure 9 were analyzed with MIP (Quanta chrome apparatus) before sending to WTCB. Table 9 shows the results.

Table 9: MIP measurements on materials with pore sizes larger then 5 µm.

Agglomerate fraction used (µm)	Pore Volume (Vol%)	Maximum Pore Size (µm)
< 125 >75	29.4	50 µm
< 180 >125	28.7	100 µm
< 500 >250	25.4	100 µm



Correction of the pore size distribution has been performed on the 50  $\mu\text{m}$  material. Results are given in figure 17 below for sample 1 (SP1 || cylinder axis) and sample 2 (SP2  $\perp$  cylinder axis). The distribution appears to be homogenous in the two directions observed.

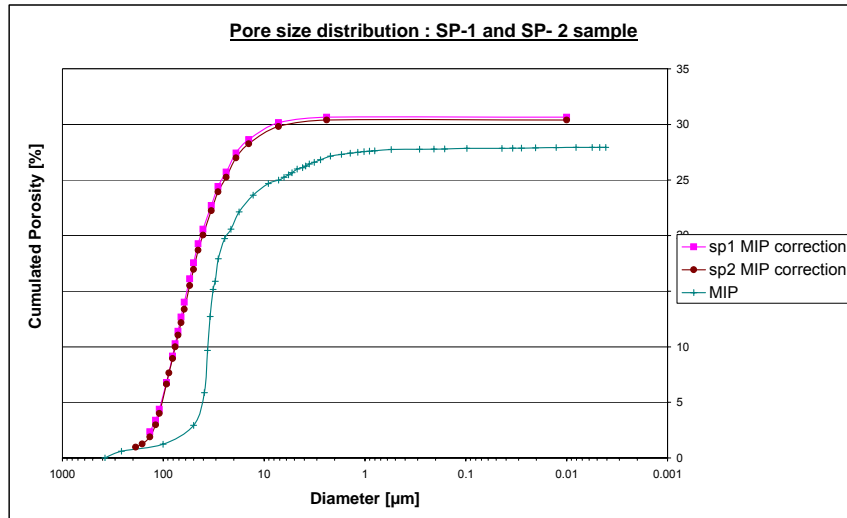


Figure 17: MIP and MIP correction for a 50  $\mu\text{m}$  material tested in two perpendicular directions (SP1 and SP2).

## 2.2.2 Application to practical problems

At the start of the program three practical programs were suggested: frost settling and water transport in building materials and the study of the drying behavior of gel casted advanced ceramic components.

Ceramic materials produced by gel casting have pore sizes of about 0.2  $\mu\text{m}$ . In view of the fact that we have concentrated the program later on, on pore size of 5  $\mu\text{m}$  or larger we have not worked anymore on that application.

The selection of reference materials with pore sizes of 50  $\mu\text{m}$  (or more) was to have a reference material simulating the broad distribution (sometimes bimodal) of the pore sizes in real building materials, and especially in clay bricks. Cylinders (high=50, diameter 20), identified hereafter by "SP", where supplied to BBRI.

Therefore, no glass spheres with nearly the same diameter were used to obtain the 50  $\mu\text{m}$  material reference material. We were persuaded that working with  $\text{Al}_2\text{O}_3$  agglomerates gives a rough but more realistic material comparable with a real clay brick.

This has been confirmed by the SEM investigations where the pore structure of the reference material has been compared with different types of clay bricks (see figure 18).

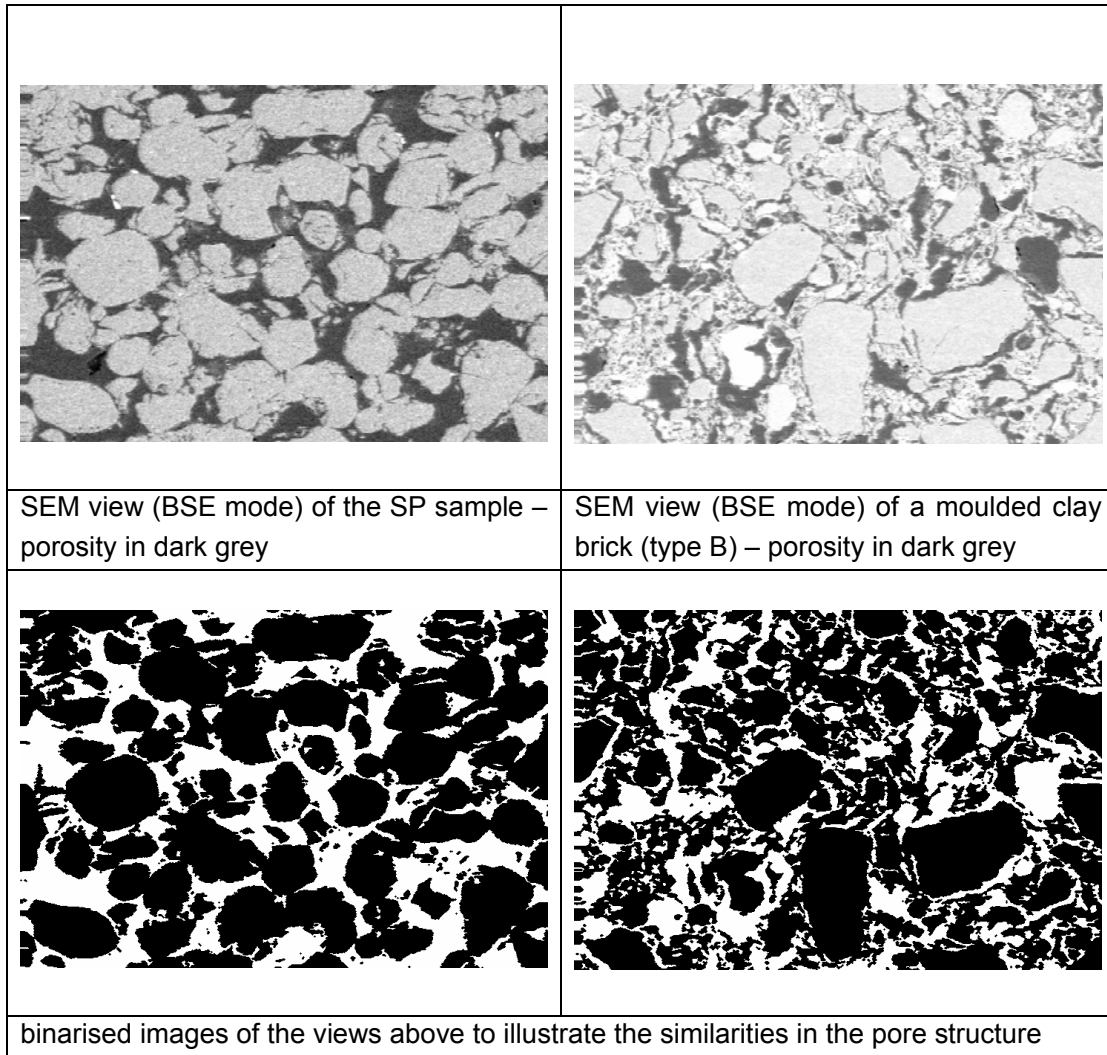
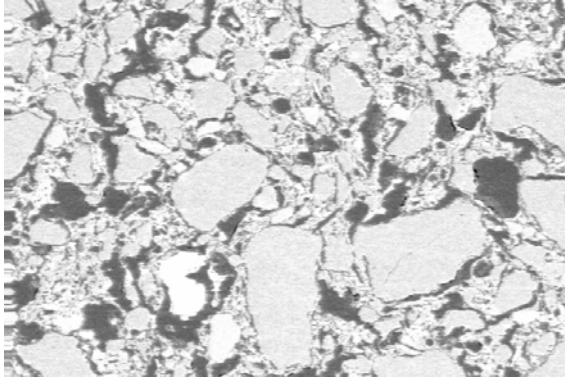
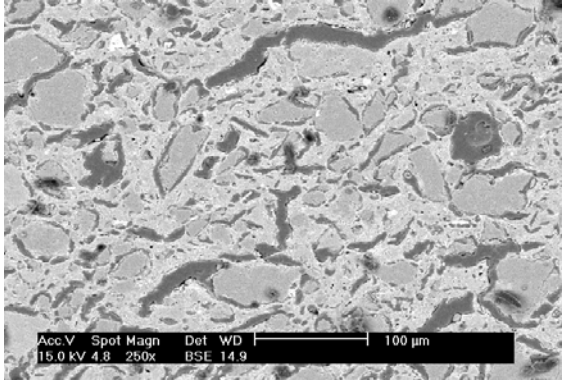
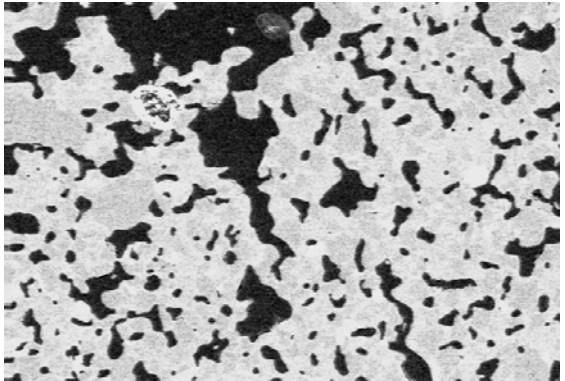


Figure 18: The comparison of the pore structure of the reference materials and the clay materials by SEM-pictures.

For this last part of the project, dedicated to applications on real materials, three types of clay bricks have been selected and their capillary behavior compared with the 50  $\mu\text{m}$  reference material prepared by VITO (identified hereafter by SP).

Their characteristics are given in Table 10.

Table 10: Characteristics of the brick materials

	type	porosity (*)	type of porosity	SEM view
brick <b>B</b>	moulded	34.00	bimodal	
brick I	extruded	17.44	bimodal (**)	
brick <b>FF</b>	moulded	28.61	bimodal	

(\*) measured by water impregnation under vacuum (vol%)

(\*\*) stretched pores parallel to the direction of extrusion

#### Pore size distribution

The PSD of the reference sample (SP) and of the 3 bricks has been determined by MIP and corrected by SEM-image analysis, according to the method described in 2.2.1.3.

The results are given in the figures 19 to 22.

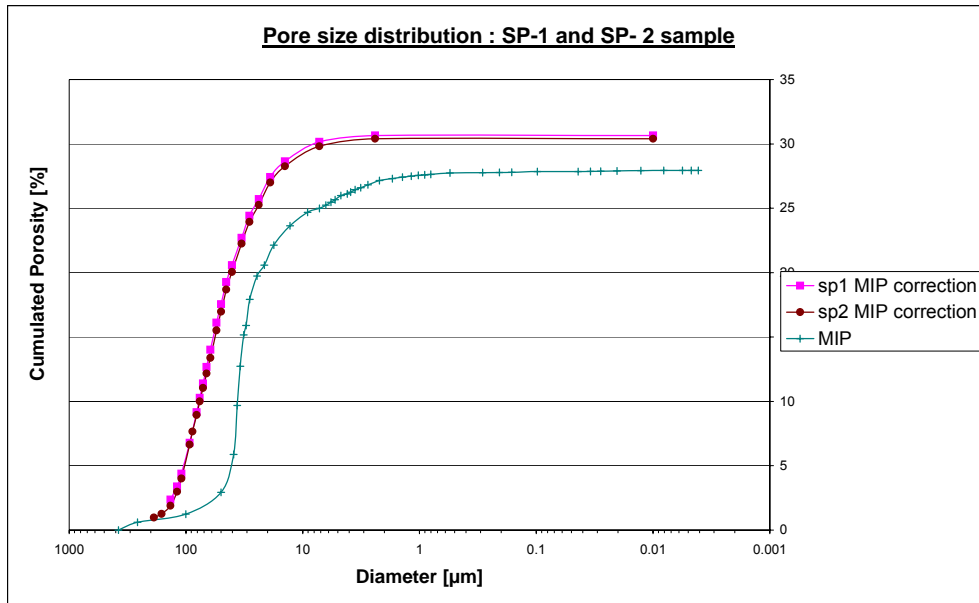
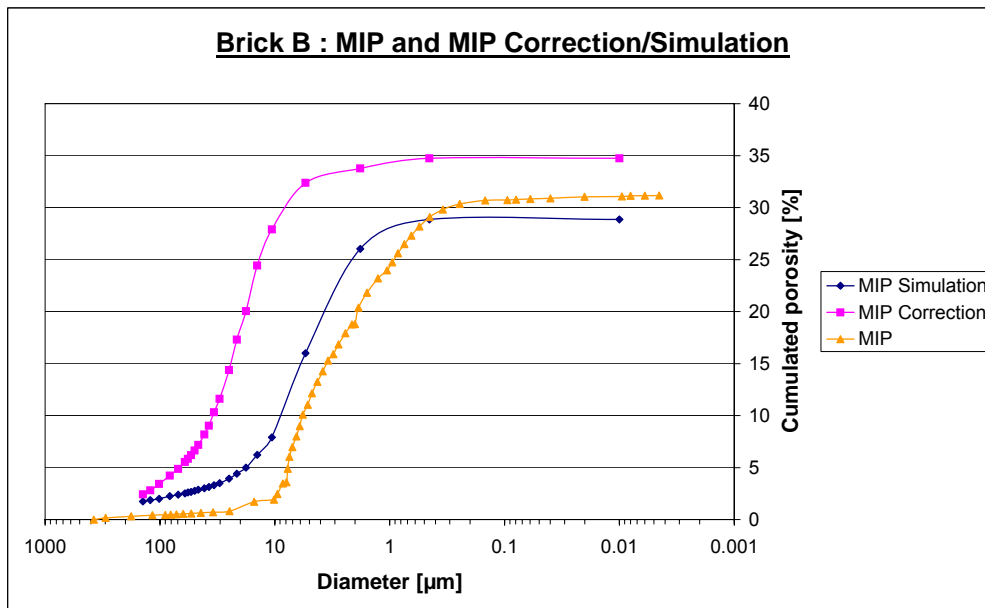


Figure 19: Pore size distribution of the reference materials SP1 and SP2 (MIP en MIP



correction)

Figure 20: Pore size distribution of Brick B (MIP, MIP simulation, MIP correction)

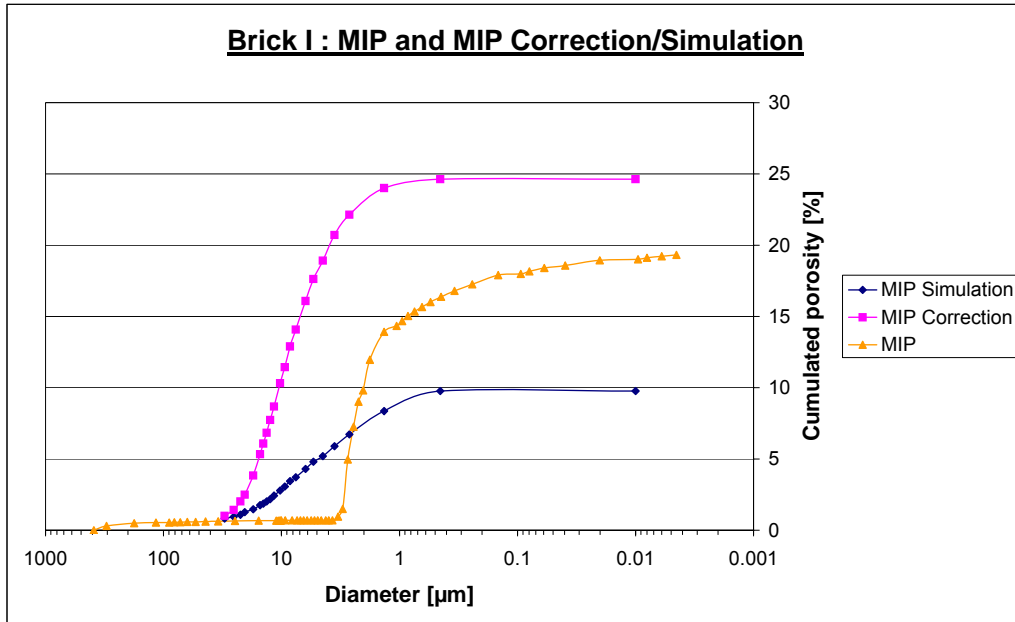


Figure 21: Pore size distribution for Brick I (MIP, MIP simulation, MIP correction)

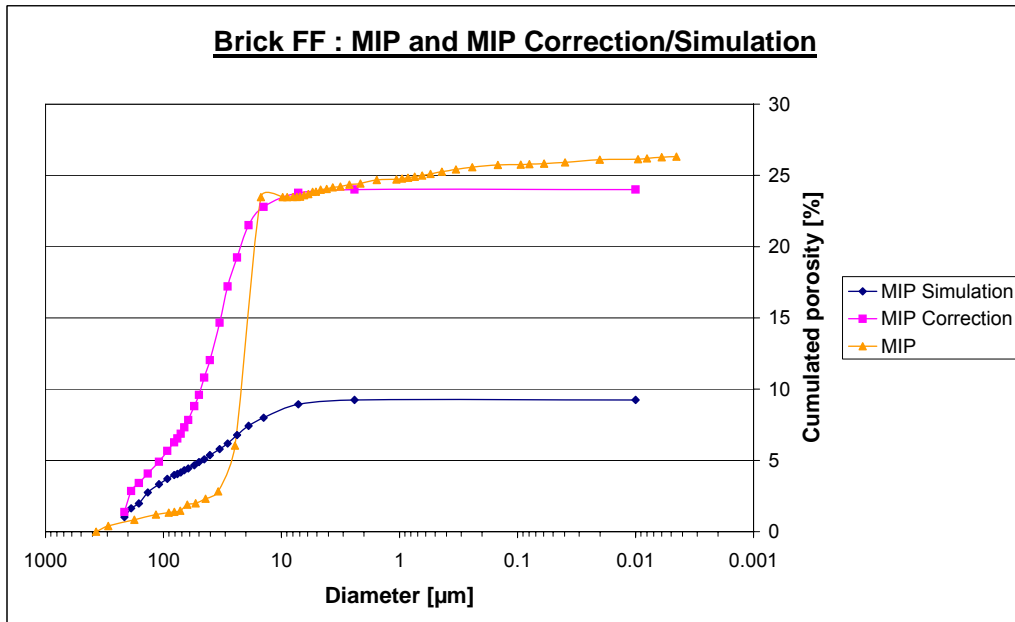


Figure 22: Pore size distribution of brick FF (MIP, MIP correction/simulation)

The following comments can be made on these results :

- The pore size distribution of the reference material and of the three different types of moulded clay bricks has been determined experimentally by MIP and by a stereological analysis of the results of automated image analysis measurements on SEM-BSE-images of polished sections. The results clearly show that the MIP pore size distribution is shifted considerably towards smaller pore diameters for all the samples, due to the well known 'inkbottle –pore' effect [19]. However, the range of this shifting varies from one brick to another. It is more important for the bricks B and I, characterized by small channels giving access to bigger pores, than for the brick FF where the distribution is not so extended. A mean pore diameter, calculated as the pore diameter corresponding to the half of the total porosity on the cumulative PSD curves, has been estimated for the experimental MIP-curves and the corrected ones. The results are summarized in table 11:

Table 11: The comparison of the mean pore diameter by MIP and MIP corrected for the reference material and the three brick materials.

sample	mean pore diameter MIP ( $\mu\text{m}$ )	mean pore diameter corrected MIP ( $\mu\text{m}$ )
SP	35	60
brick B	3.1	21.4
brick I	2.1	8.5
brick FF	23.8	40.4

We see that the effect of the correction on the mean pore size is also very important.

- The simulation of the mercury intrusion gives for the bricks I and FF results which are not coherent with the experimental curves. Especially, the volume of the invaded porosity during the simulation is too small. On the other hand, the obtained result for the brick B seems to be more logical. The reason for this is that the brick B is characterized by a high porosity and an important connectivity between the pores. With this kind of pore structure, the risk is low to have isolated pores or isolated clusters of pores on a 2-dimensional representation of the microstructure. This is not the case for the bricks I and FF where the porosity and the pore-connection is lower. This point should be refined in a further study, taking into account the problem of the connectivity between the pores and its evaluation on a 2D-representation of pore structure.

### Capillary water absorption

Experimental procedure :

The capillary water absorption of building materials can be characterized by a simple test method. The method described hereafter is the one used in different EN standards (for clay bricks or natural stone) [20-22] and does not differ much from the capillary rise absorption test recommended by RILEM.

After drying to constant mass, the base of the samples is immersed in water on one of its sides and the increase of weight is measured in function of time. The mass of water absorbed ( $m$ ) divided by the horizontal area ( $A$ ) of the base of the specimen ( $\text{g/m}^2$ ) is plotted on a chart against the square root of time until the rising water reaches the top of the sample. Usually, the absorption is characterized by two straight lines. The slope of the first one is relative to the velocity of the capillary absorption. The second one, showing a very slow increase of the sample's weight, corresponds to the filling of very small pores and to the diffusion of the entrapped air in the pore structure which can lead to an increase of the saturation up to nearly 100% of the total porosity after a very long time. This diffusion process has not been taken into account here.

Another way to show the results of the absorption test is to plot the water absorption expressed in percentage of the total porosity. In this way, the capillary saturation level, that is the percentage of the porosity of a material that can be filled with water by natural absorption, can be easily estimated as the intercept of the two lines. This capillary saturation level (called  $S\%$ ) is a very important characteristic of building materials, as it conditions for example the frost resistance [23].

For the determination of the capillary behavior of the samples prepared by VITO, the test method has been adapted to the small sizes of the samples. The cylinder to test (high = 50 mm, diameter 23 mm) is hanged to a hoop supported by the plate of the laboratory balance (see figure 20). A small water container independent of the plate is put under the hanging sample and the water level is adjusted in order to have an immersion of 3 mm of the base of the sample.

The increasing weight is recorded automatically all the 5 seconds by a computer connected to the balance.



Figure 23: Test apparatus for measuring the capillary behavior of the porous samples.

The results are shown in figure 24.

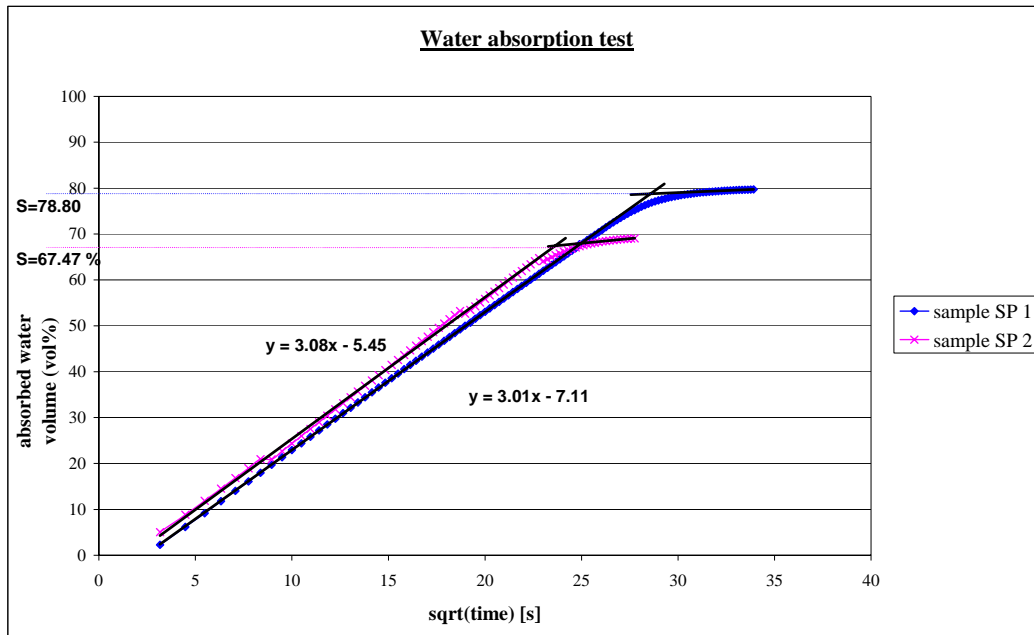


Figure 24: The water absorption test for the reference materials.

The fact of having two perfectly straight lines confirms that the homogeneity of the pore structure from the base to the bottom of the samples is quite good.



The same experiment has been carried out for the three clay bricks (figure 25).

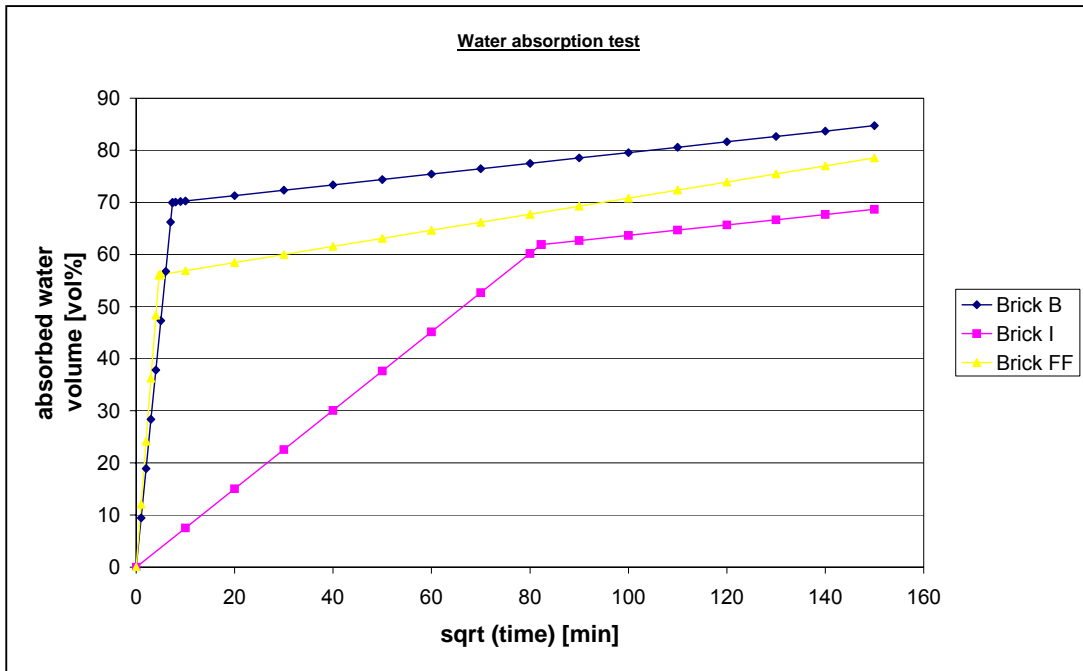


Figure 25: The water absorption test for the three bricks

The capillary behavior of porous materials is completely determined by their pore structure. Particularly, two important pore structure characteristics are considered as crucial :

- the size of the pores which will determine the rate of the absorption, according to the following relation (Washburn-Poiseuille) :

$$h(t) = \sqrt{\frac{\sigma \cdot \cos\theta}{2 \cdot \eta}} \cdot \sqrt{r} \cdot \sqrt{t} \quad [24]$$

where : h = height of the wetting front

$\sigma$  = surface tension of water

$\theta$  = contact angle between water and material

$\eta$  = viscosity of water

r = radius of the capillary

- the spreading of the PSD which will influence the quantity of air entrapped in the microstructure during the water invasion. A very broad PSD combining very fine pores with larger ones will give the most chances to entrap the air in the porosity during water absorption, resulting in a low capillary saturation level. On the other hand, a narrow and sharp PSD will give an homogenous filling of the pores with water, no trapping of the air and consequently a high capillary saturation level. This phenomenon has been confirmed by the following experiment in BBRI : a sample of brick with a bimodal distribution of pores has been impregnated by

capillarity with a yellow epoxy resin [25]. After polymerization, the empty porosity has been impregnated under vacuum with a blue resin. A thin section has then been realized in order to observe which pores have been filled in yellow or in blue. The observations under an optical microscope clearly show that the capillary active pores, collared in yellow, are the smallest ones and that the bigger ones are all filled in blue, meaning they are not capillary active and they will stay empty (filled with air) during a real water absorption (figure 26).

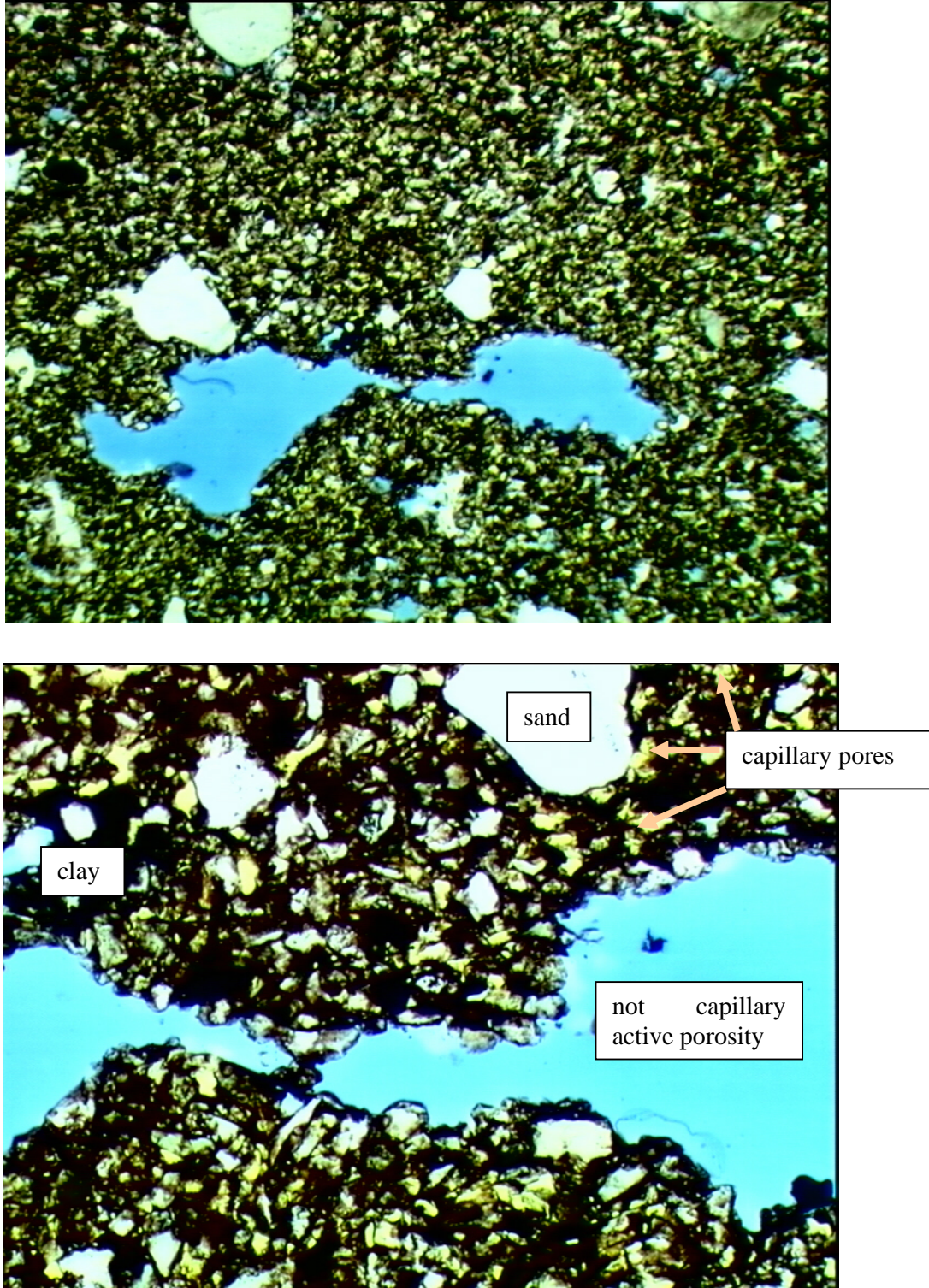


Figure 26: Optical micrograph showing capillary active and non-active pores.

Thanks to our method for measuring the true PSD, we have been able to confirm and give more details about these experimental observations.

For example, the similarities between the corrected PSD of the bricks B and FF (see figure 27) are confirmed by the capillary results (the absorption rates are nearly the same).

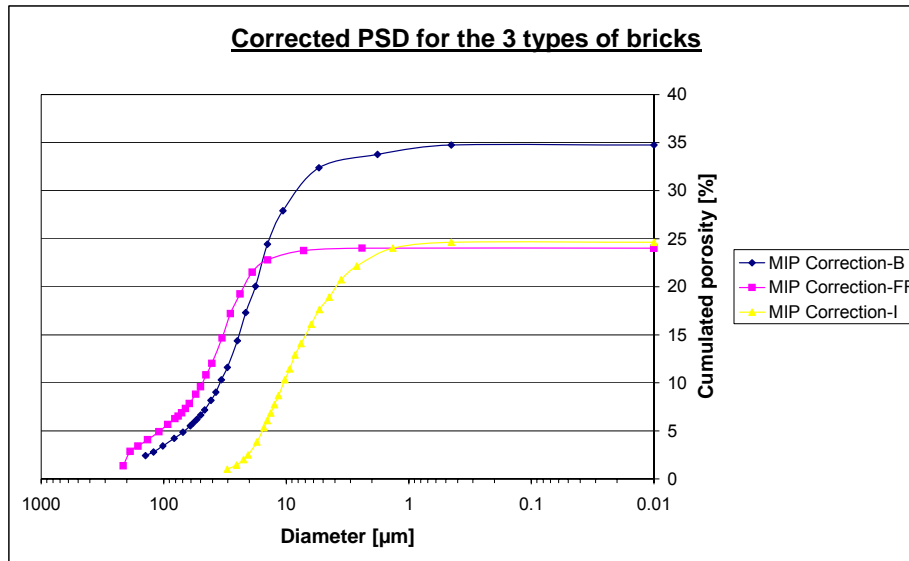


Figure 27: The corrected MIP pore size distributions for the three bricks.

Moreover, the following relation has been found between the rate of absorption and the size of the mean pore, table 12 and figure 28.

Table 12: The experimental relation between rate of absorption and the mean pore size as found for the 4 materials

sample	capillary saturation level (S%)	rate of absorption (g/m <sup>2</sup> /√s)	mean pore diameter corrected MIP (μm)
SP	73	972	60
brick B	71%	422	21.4
brick I	62%	18	8.5
brick FF	56%	433	40.4

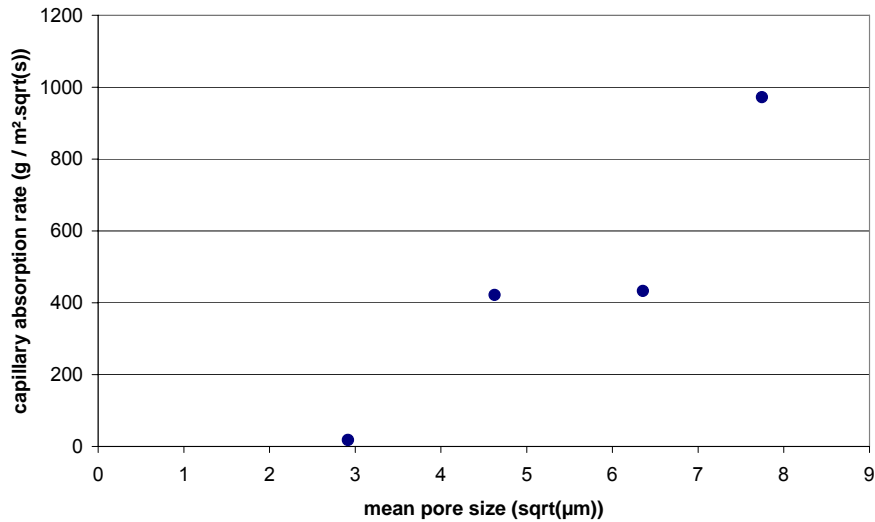


Figure 28: The capillary absorption rate as a function of (the mean pore size)<sup>1/2</sup>

This is in good agreement with the relation of Washburn-Poiseuille given above and will permit in the future, when more points will be available, to have an experimental evaluation of the constant values of the relation and by this way, to predict the capillary behavior of a material on the basis of its PSD.

### 2.2.3 Conclusions of Part 2

1. Reference materials with pore size of 5  $\mu\text{m}$  and 100  $\mu\text{m}$  could be produced (bimodal) in a reproducible way.
1. Water absorption tests prove that their structure is homogeneous.
2. MIP and IA-measurements were optimized for this kind of materials.
3. The pore size distribution measured by MIP can be corrected for its “bottle neck” effect based on IA of SEM pictures.
4. The method could be applied successfully on a few real brick materials.
5. An onset was made to study the water transport behavior in brick materials.

## 3 RESULTS OF THE PROJECT

1. Manufacturing routes for porous references for the whole range of pore sizes were worked out.

For the materials used in the pore size range of 3 to 15 nm, we produced flakes by a sol gel method. A Reaction Bonded  $\text{Al}_2\text{O}_3$  manufacturing route could be used to produce strong materials with pore sizes between 0.15 $\mu\text{m}$  and 10  $\mu\text{m}$ .

The pore size range of 10 to 100  $\mu\text{m}$  can be covered by a system where large agglomerates are mixed with 5 to 10 wt% of fine powder and synthesized by pressing and sintering. Finally, materials with pore sizes bigger than 100 $\mu\text{m}$  can be produced by ceramic foam techniques.

- MIP measurements can only be done for pore sizes between 6 nm and 0.3 mm. This was a first limitation. Sol gel and ceramic foam techniques are therefore excluded. Later on after a year, we decided to concentrate on pore sizes between 5 and 100  $\mu\text{m}$ , because there are no reference materials of BAM in that pore-size range.
2. The different materials originally produced were tested with different analytical techniques and compared to MIP measurements.  
MIP measurements were performed with two apparatus to optimize the materials, their structure, their shape and volume and the way of measurement.  
Very reproducible materials could be produced.
  3. The same materials were also extensively study by Image Analyze and a method was worked out to correct MIP measurements with a model based on Image analysis measurements.
  4. The obtained techniques and their interpretation were demonstrated on materials with pore sizes between 5 and 100  $\mu\text{m}$  and on a few real brick materials with a well known pore structure.
  5. An onset was made to study the water transport behavior in brick materials.
  6. A paper [26], describing the first part of the project, was already published in Key Engineering Materials, vols 206-213 (2002) p681  
J. Luyten, A. Buekenhoudt, F. de Barquin and J. Elsen  
"Reference Materials for adequate porosity measurements."

#### 4 SPREADING AND VALORISATION

In this project we demonstrated that porous reference materials can be produced in a reproducible way, without using artificial materials as glass spheres. Moreover, using MIP combined with IA, a new basis was obtained for the interpretation of porous materials in general, especially in the pore size range between 0.2  $\mu\text{m}$  and 100  $\mu\text{m}$ .

The lower pore size range, pore size from 6 nm to 5  $\mu\text{m}$  is certificated or will be certificated soon by BAM based on  $\text{N}_2$ -adsorption - or MIP measurements. The pore size range up to 5  $\mu\text{m}$  is still open for certification. In this project, in view of the budget and time, we did not have the possibilities to do the whole referencing procedure as done by BAM for the lower pore size range. But, probably we have produced sufficient results for working out an isonorm for large pore sizes in a program together with BAM in the future. Samples are exchanged as a start.

For materials with pore sizes above 5  $\mu\text{m}$  the "bottle neck effect" of the MIP measurements, and therefore the developed method of correction of the MIP pore distribution, is much more important then for the small pore sizes. This method opens a lot of new perspectives for as well scientific as well technological applications.

Most building materials have a bimodal pore size distribution, with relative small pores (less then 5  $\mu\text{m}$ ) and large pore sizes (between 30 and 200  $\mu\text{m}$ ). Such a bimodal ceramic structure was developed and characterized in this project. In this way, the producers of building materials have now a fast tool for the correct measurement of the pore size. It will allow them to correct their production and to prevent problems as frost settling.

Moreover, in the future, water transport and others in building materials can be studied more accurate using this work.

Vito and WTCB/CSTC has the attention to continue the collaboration on this topic and to publish a few papers together in the near future.

## **5 BALANCE AND PERSPECTIVES**

The main objectives of the project are realized:

- Porous references materials could be manufactured in a large range of pore sizes. They were measured with different analyzing techniques to compare their results with MIP measurements.
- MIP results on the optimized materials proved that the porous materials can be manufactured in a reproducible way, a requirement for a reference material.
- The basis idea of the whole project- the correction of MIP measurements by a model based on IA-measurements –could be realized
- The practical applications as foreseen in the original objectives are only partially realized. As mentioned earlier, after a year we decided to concentrate on pore sizes between 5 and 100  $\mu\text{m}$ , as advised by the steering committee therefore the practical application concerning the gel casting of ceramics, aiming at pore sizes of 0.2  $\mu\text{m}$ , fell. However, for building materials the developed correction method was successfully applicated and an onset was made to study the water transport behavior in brick materials as foreseen in the original objectives. This part has to be worked out more extensively in the future, because together with the knowledge of the right pore size distribution, it forms the basis for solving the frost settling in brick materials [27].

## **6 ACKNOWLEDGEMENT**

The authors want to thank the people of the users committee:

Prof. Kl. Meyer, BAM (D)

Dr.ir. L. Jacobs, N.V. Bekaert S.V.

Ir. N. Lens, Koramic Building products

Ing. F. Devreese, Ankersmid

The discussions on the different meetings were very helpful and gave us the possibility to steer our project in the good direction. We received a lot of technical documentation and practical advice during these two years.

Especially, we want to express our acknowledgement to the people of BAM who send us results, measured on comparable materials.

## **7 REFERENCES**



1. J. Luyten, J. Cooymans, C. Smolders, S. Vercauteren, E.F. Vansant and R. Leysen, "Shaping of multilayer ceramic membranes by dip coating", *J. Eur. Ceram. Soc.*, 17 pp. 273-279 (1997)
2. S. Vercauteren, K. Keizer, E.F. Vansant, J. Luyten and R. Leysen, "Porous ceramic membranes: preparation, transport properties and applications", *J. Porous Mat.*, 5, pp. 241-258 (1998)
3. N. Claussen, Tuyen Le and Suxing Wu, "Low shrinkage reaction-bonded alumina", *J. Eur. Ceram. Soc.* 5, pp. 29-35 (1989)
4. J. Luyten, J. Cooymans and R. Leysen, "Shaping of a RBAO membrane support", *Key Engineering Materials*, pp. 132-136, *Euro Ceramics V*, 3, pp. 1691-1694 (1997)
5. P. Omatete, M. Janney and R. Strehlow, "Gel casting - a new ceramic forming process", *Ceram.Bull.*70, pp. 1641-1649 (1991)
6. R. Gilissen, J.P. Erauw, A. Smolders, E. Vanswijghoven and J. Luyten, "Gel casting, a near net shape technique" *Materials and design* 21, (2000), pp. 251-257
7. J. Shaep, C. Vandecasteele, B. Peeters, J. Luyten, C. Dotremont and R. Roels, "Characteristics and retention properties of a mesoporous  $\gamma$ -Al<sub>2</sub>O<sub>3</sub> membrane for nanofiltration", *J. Membrane Sci.*, 163 , pp. 229-237 (1999)
8. F. Andreola, C. Leonelli, M. Romagnoli and P. Miselli, "Techniques used to determine Porosity", *Amer. Ceram. Soc. Bull.*, July 2000, pp. 49-52
9. Iso-norms about MIP kindly supplied by Mr. F. Devreese (Ankersmid)
10. Different BAM documents about MIP, gas absorption and reference materials, kindly supplied by Prof. Kl. Meyer (BAM)
11. J. Elsen and F. de Barquin, "Modeling of the capillary water absorption of porous building materials", To be published.
12. M. Coster and J-L. Chermant, "Précis d'analyse d'images", Ed. Presses du CNRS, 1989
13. C. Stein, "Two-sample test of a linear hypothesis whose power is independent of the variance", *Ann. Math.* 16, pp. 243-258 (1945)
14. SK. Chatterjee, "Two-stage and multistage procedure", in *Handbook of Sequential Analysis*, 21-45, Marcel Dekker, New-York (1991)
15. ASME B46.1, "Surface texture (surface roughness, waviness, and lay)", The American Society of Mechanical Engineers (1993)
16. M. Maage, "Frost resistance and pore size distribution in bricks", *Mat. et Constr.*, vol 17, n°101, pp. 345-350.
17. A. Ammouche, "Caractérisation automatique de la microfissuration des bétons par analyse d'images", Thèse n°2180 , Univ. Bordeaux I (1999)



18. L. Daian and D. Quenard, "Invasion and transport processes in multiscale model structures for porous media", IUPAC, Symp. on the Charact. of Porous Media, 1993
19. F. Metz, "Systematic mercury porosimetry investigations on sandstones", *Materials and Structures*, 25, (1992)
20. EN 1925, "Natural stone – Test methods - Determination of water absorption coefficient by capillarity", CEN (1999)
21. B. Meng, "Moisture-transport-relevant characterization of pore structure", Proc. of the 6<sup>th</sup> Int. Congress on Deterioration and Conservation of stone, Liboa, pp. 387-396 (1992)
22. C. Hall, "Water movement in porous building materials", *Building and Env.*, v 22, n°1, pp. 77-82
23. R. Gérard, "Détermination de la durabilité au gel par une méthode de capillarité", Proc. of the 5<sup>th</sup> Int. Congress on deterioration and conservation of stone, Lausanne (1985) pp. 157-165
24. J. Szekely, AW. Neumann and YK. Chuang, "The rate of capillary penetration and the applicability of the Washburn equation", *Journal of Colloid and Interface Science*, vol.35, n°2 (1971)
25. B. Zinszner and Ch. Meynot, "Visualisation des propriétés capillaires des roches réservoir", *Revue de l'Inst. Français du Pétrole*, v 37, n°3, pp. 337-361
26. J. Luyten, A. Buekenhoudt, F. de Barquin and J. Elsen, "Reference Materials for adequate porosity measurements", *Key Engineering Materials*, vols 206-213, p. 681 (2002)
27. M. Sveda, "Frost resistance of brick", *Amer.Ceram.Bull.*, Vol.80, No 9, pp. 46-48

Uitgegeven in 2005 door het Federaal Wetenschapsbeleid

De wetenschappelijke verantwoordelijkheid over de inhoud van dit eindverslag berust volledig bij de auteurs.

---

**FEDERAAL  
WETENSCHAPSBELEID**

Wetenschapsstraat 8 ■ B-1000 BRUSSEL  
Tel. 02 238 34 11 ■ Fax 02 230 59 12  
[www.belspo.be](http://www.belspo.be)

